

## Structural basis for the inhibition of Aurora A kinase by a novel class of high affinity disubstituted pyrimidine inhibitors

Leslie W. Tari,<sup>a</sup> Isaac D. Hoffman,<sup>a</sup> Daniel C. Bensen,<sup>a</sup> Michael J. Hunter,<sup>a</sup> Jay Nix,<sup>b</sup> Kirk J. Nelson,<sup>a</sup> Duncan E. McRee<sup>a</sup> and Ronald V. Swanson<sup>a,\*</sup>

<sup>a</sup>ActiveSight, 4045 Sorrento Valley Blvd., San Diego, CA 92121, USA

<sup>b</sup>Advanced Light Source, Beamline 4.2.2, 1-Cyclotron Rd., Berkeley, CA 94720, USA

Received 11 September 2006; revised 27 October 2006; accepted 30 October 2006

Available online 2 November 2006

**Abstract**—The 2.25 Å crystal structure of a complex of Aurora A kinase (AIKA) with cyclopropanecarboxylic acid-(3-(4-(3-trifluoromethyl-phenylamino)-pyrimidin-2-ylamino)-phenyl)-amide **1** is described here. The inhibitor binding mode is novel, with the cyclopropanecarboxylic acid moiety directed towards the solvent exposed region of the ATP-binding pocket, and several induced structural changes in the active-site compared with other published AIK structures. This structure provides context for the available SAR data on this compound class, and could be exploited for the design of analogs with increased affinity and selectivity for AIK. © 2006 Elsevier Ltd. All rights reserved.

The Aurora family of serine/threonine kinases are essential for mitotic progression. Mammals express three paralogs; Aurora A, Aurora B, and Aurora C. The three enzymes share highly similar catalytic domains, but show different subcellular localization.<sup>1</sup> Aurora A is essential for mitotic spindle formation and accurate chromosome segregation, while Aurora B is a chromosome passenger protein kinase that regulates centrosome separation, chromosome segregation, and cytokinesis.<sup>2</sup> Overexpression of Aurora kinases results in chromosomal instability, suggesting that Aurora kinase may be of potential importance in cancer. Indeed, a causal link has been established between the overexpression of Aurora A and B kinases, and tumor progression.<sup>3–5</sup> Specific, potent inhibitors of Aurora A and B kinases, such as VX-680, have been shown to be so effective at suppressing tumor growth in vivo that they have progressed into clinical trials.<sup>6</sup> The validation of Aurora kinases as drug targets has spawned a flurry of activity over the last several years, directed towards the discovery of novel Aurora kinase inhibitors with potential value as anti-cancer drugs.<sup>7–9</sup> In this report, we describe the crystal structure of AIKA complexed with cyclopropanecarboxylic acid-(3-(4-(3-trifluoromethyl-phenylamino)-

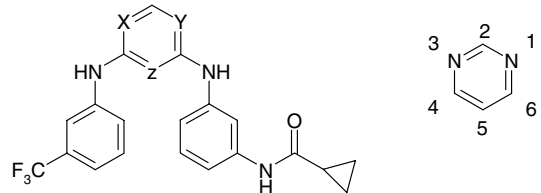
pyrimidin-2-ylamino)-phenyl)-amide **1**, and discuss the implications of this structure in the context of the available SAR data for analogs of compound **1**.

Disubstituted pyrimidines, particularly with aniline substituents at the 2 and 4 positions, have been explored fairly extensively as potential inhibitors of kinases from the receptor and non-receptor tyrosine kinase and serine/threonine kinase families.<sup>11–13</sup> Crystallographic studies have revealed a common binding mode for 2,4-dianilinopyrimidines in the nucleotide-binding pocket: The inhibitors typically interact with the kinase via a pair of hydrogen bonds with backbone atoms in the kinase hinge region, utilizing an aniline proton and a pyrimidine nitrogen.<sup>14</sup> Despite the generic nature of the core interaction, it is possible to achieve a considerable range of selectivity profiles of 2,4-dianilinopyrimidines by altering the substitution pattern on the pendant aniline rings.

Compounds **1–3** were synthesized from a combinatorial library in an effort to discover potent, specific inhibitors of EGFR.<sup>10</sup> While compound **3**, a 4,6-disubstituted pyrimidine, potently inhibited EGFR (IC<sub>50</sub> 21 nM) in a selective manner, the 2,4-regioisomers (compounds **1** and **2**), only weakly inhibited EGFR (IC<sub>50</sub> > 10,000 nM), while strongly inhibiting AIKA (Table 1). To address these selectivity issues, and to understand the basis for

**Keywords:** Aurora; AIK; Kinase; 2,4 Disubstituted pyrimidine.

\* Corresponding author. Tel.: +1 858 229 3716; fax: +1 858 455 6932; e-mail: [rswanson@active-sight.com](mailto:rswanson@active-sight.com)

**Table 1.** In vitro SAR of disubstituted pyrimidine analogs<sup>a</sup>


Compound	X	Y	Z	AIKA IC <sub>50</sub> (nM)
<b>1</b>	C	N	N	42
<b>2</b>	N	C	N	931
<b>3</b>	N	N	C	>10,000

<sup>a</sup> Data extracted from reference 10.

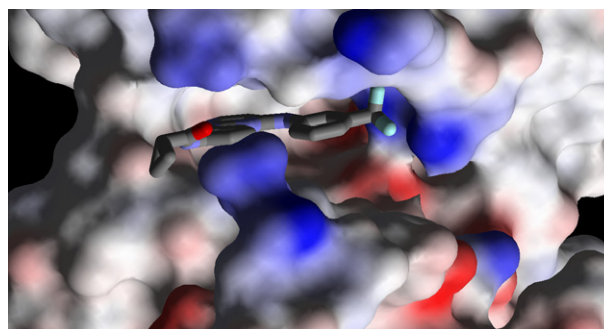
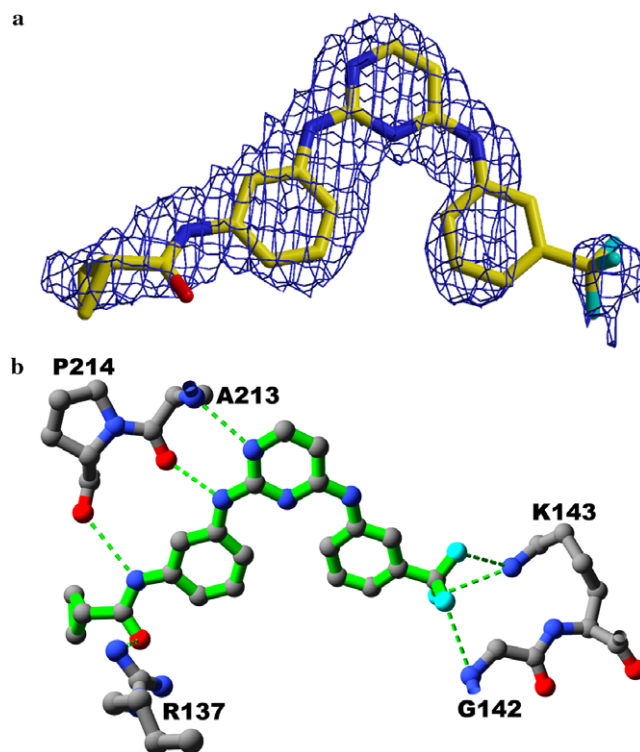
high affinity binding of the 2,4-regioisomers to AIKA, we determined the crystal structure of AIKA complexed with **1**.

Crystals diffracting to 2.25 Å (Table 2) were obtained from recombinantly expressed AIKA complexed with **1**.<sup>15</sup> The structure of the title complex was determined using the structure of the catalytic domain of AIKA with ATPγS<sup>16</sup> as a molecular replacement model.<sup>17</sup>

The title complex<sup>18</sup> possesses a prototypical bilobal kinase catalytic domain structure, with a long, deep nucleotide binding cleft that is occupied by the inhibitor (Fig. 1). Electron density is visible for residues 127–388, with the exception of a portion of the activation loop comprising residues 286–291, which is dynamically disordered. In terms of its gross features and the relative orientations of the N- and C-terminal domains, the structure of the title complex is similar to the other published structures resembling the activated form of Aurora A kinase.<sup>16,19,20</sup> However, the N- and C-terminal domains are rotated towards one another by approximately 10° when compared to their counterparts in the structure of the inactivated form of Aurora A kinase.<sup>8</sup>

Compound **1** adopts an *s*-cis conformation upon binding to AIK (Fig. 2a), exposing most of the available hydrogen-bonding groups on the inhibitor to the interior of the active-site. The dipyrimidine and aniline

moieties bind in a classical adenine mimetic fashion, forming two hydrogen bonds with main chain atoms from A213 in the hinge region. The cyclopropylamide

**Figure 1.** Solvent accessible surface of the AIKA-compound **1** complex, colored by electrostatic surface potential (blue-positive, red-negative). The N-domain is at the top. The nucleotide binding cleft is expansive, spanning the entire width of the protein. The hinge region is located in the deepest recesses at the back of the binding pocket. Favorable electrostatic interactions are observed between active-site residues and the trifluoromethyl group, as well as the cyclopropylamide.**Figure 2.** Detailed views of the conformation of compound **1** and its binding mode to AIK. (a) refined omit *F<sub>o</sub>-F<sub>c</sub>* (2.5σ) difference electron density map showing the conformation of the inhibitor. The electron density is discontinuous across the trifluoromethyl-phenyl group and the group's thermal factors are larger than those for the rest of the inhibitor, indicating a high degree of thermal motion in the phenyl group. The trifluoromethyl group occupies a large, open pocket in the active-site, and binds intrinsically mobile residues in the p-loop; (b) detailed schematic showing the hydrogen-bonding network between compound **1** and the active-site. The inhibitor is shown with green bonds, and potential hydrogen bonds are depicted as green dotted lines. The cyclopropyl group is exposed to solvent.**Table 2.** Crystallographic data and refinement statistics

AIKA-compound <b>1</b>	
Space group	P6 <sub>1</sub> 22
Unit cell parameters	81.54, 81.54, 172.04 Å, 90°, 90°, 120°
Total reflections	66,089
Unique reflections	16,671
Rsym <sup>a</sup>	7.6% (48.2%)
Resolution	54.58–2.25 (2.33–2.25) Å
<i>I</i> /σ( <i>I</i> )	8.6 (1.8)
Completeness	99.4% (99.9%)
<i>R</i> <sub>(work)</sub> , <i>R</i> <sub>(free)</sub> <sup>b</sup>	24%, 28%
Rmsd bonds	0.008 Å
Rmsd angles	1.1°

<sup>a</sup> Numbers in parentheses refer to data in the highest resolution shell.<sup>b</sup> 5% of the data were excluded from the refinement for the calculation of *R*<sub>(free)</sub>.

is oriented away from the catalytic machinery of AIK and partially solvent exposed, engaging the main chain carbonyl of P214 and the R137 side chain in hydrogen-bonding interactions (Fig. 2b). The trifluoromethyl group interacts with the G142 main chain as well as K143 in the p-loop.

The binding of **1** to AIKA induces a number of conformational changes in the protein (compared with other published structures), illustrating the inherent plasticity of the AIKA active-site. The most dramatic changes are observed in the p-loop (residues 140–145) and the DFG motif in the activation loop (residues 274–276, Fig. 3). The relative orientations of the p-loops in the title structure and the structure of activated nucleotide bound AIK are distinctly different; the typically observed  $\beta$ -hairpin conformation of the p-loop is distorted and the main chain in the AIKA-compound **1** complex rotates towards the active-site cleft by 1.7 Å and N $\epsilon$  of K143 swings by 9 Å towards the hinge region, where it is positioned to interact with the trifluoromethyl moiety of the inhibitor. Also, the DFG motif adopts a conformation that is structurally distinct from its counterparts in the other published structures of Aurora A kinase. In the overlaid structures, the root-mean-squared-differences between the atomic positions of the atoms in residues A273–S278 are 3.2 and 5.6 Å, respectively, when comparing the title structure to the structures of phosphorylated, activated (DFG-in) AIK<sup>19</sup> and inactive (DFG-out) inhibitor bound AIK.<sup>8</sup> On the basis of this analysis, the AIKA-compound **1** complex structure more closely resembles the activated form of AIK.

The relative positioning of the cyclopropylamide from **1** in the kinase active-site is unique, when compared to other published kinase-inhibitor complex structures describing inhibitors utilizing terminal hydrophobic amide substituents. In the structures of Abl complexed with VX-680 (which also contains a terminal cyclopropylamide substituent),<sup>21</sup> and the structure of AIK complexed with a 5-aminopyrimidinyl quinazoline containing a terminal benzamide,<sup>8</sup> the hydrophobic amide substituents are bound deep in the kinase active-site, where they interact with residues from the DFG-motif.

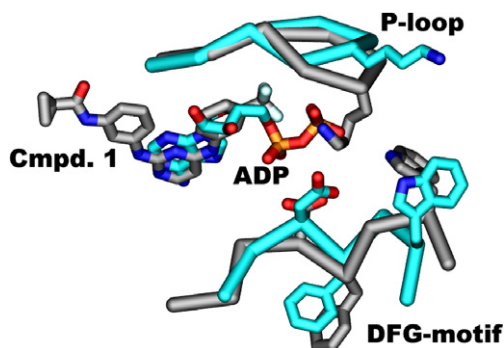


**Figure 3.** Overlay of the complex of AIK with **1** (grey carbons) with the structure of activated, nucleotide bound AIK (blue carbons).<sup>19</sup> In the title structure, K143 of the p-loop occupies the same position as the  $\beta$ -phosphate of ADP. W277, adjacent to the DFG-motif, twists away from the active-site cleft.

In the case of the 5-aminopyrimidinyl quinazoline compound, the benzamide stabilizes an inactive form of AIK by locking the DFG motif in a non-productive conformation.<sup>8</sup> In the title structure, the thermodynamically favored binding mode positions the CF<sub>3</sub> group close to the DFG motif, with the cyclopropylamide binding productively to a kinase hinge residue and a surface arginine (Fig. 2b). The relative positioning of the cyclopropylamide near the protein surface in this structure provides a likely explanation for the lack of selectivity of compound **1** for AIK (IC<sub>50</sub>s of <900 nM were observed for 9 kinases out of a panel of 55 with compound **1**, including BmX, LcK, IGF-1R, and Syk.<sup>10</sup>) when compared to the selectivity profiles of VX-680<sup>22</sup> and the benzamide substituted 5-aminopyrimidinyl quinazolines described above.<sup>8</sup> It is reasonable to hypothesize that a compound's selectivity for AIK is correlated with its tendency to induce an inactive DFG-out kinase conformation. Thus, the selectivity profiles and affinities of analogs of compound **1** for AIK may be increased through elongation of compound **1** at the CF<sub>3</sub> site (extending it into the DFG region), while retaining a functional group at the CF<sub>3</sub> position that exploits the favorable electrostatic interactions with the active-site.

The structural analysis of the title complex provides insights into the in vitro SAR data for analogs of compound **1** (Table 1). The loss of affinity observed in compound **2** is likely due to the loss of the hydrogen bond observed between compound **1**, and the amide nitrogen of A213 (Fig. 2b). No potential hydrogen bond donors are within range of a pyrimidinyl nitrogen ortho to the trifluoromethylphenyl substituent. The dramatic loss in affinity observed for compound **3**, a 4,6 disubstituted pyrimidine, can likely be ascribed to the greater energetic penalty such a compound would incur to adopt the s-cis conformation required for interaction with the AIK hinge region.

In summary, we have characterized a novel binding mode for a newly discovered 2,4-disubstituted pyrimidine inhibitor of AIK. The structure provides context for the SAR data on analogs of compound **1**, and insights into the active-site plasticity of AIK. This complex structure also provides an excellent basis for the design of more specific and potent analogs of **1** with potential therapeutic value in the treatment of cancer.

### Acknowledgments

We gratefully acknowledge Dr. Edwin Westbrook and the staff at beamline 4.2.2 at the Advanced Light Source for their assistance with this project.

### References and notes

1. Carmena, M.; Earnshaw, W. C. *Nat. Rev. Mol. Cell Biol.* **2003**, *4*, 842.
2. Lee, E. C. Y.; Frolov, A.; Li, R.; Ayala, G.; Greenberg, N. M. *Cancer Res.* **2006**, *66*, 4996.

3. Bischoff, J. R.; Plowman, G. D. *Trends Cell Biol.* **1999**, *9*, 454.
4. Bischoff, J. R.; Anderson, L.; Zhu, Y.; Mossie, K.; Ng, L.; Souza, B.; Schryver, B.; Flanagan, P.; Clairvoyant, F.; Ginther, C.; Chan, C. S. M.; Novotny, M.; Salomon, D. J.; Plowman, G. D. *EMBO J.* **1998**, *17*, 3052.
5. Giet, R.; Prigent, C. *J. Cell Sci.* **1999**, *112*, 3591.
6. Mortlock, A. A.; Keen, N. J.; Jung, F. H.; Brewster, A. G. PCT Int. Appl. WO 2001021596, **2001**.
7. Mortlock, A. A.; Keen, N. J.; Jung, F. H.; Heron, N. M.; Foote, K. M.; Wilkinson, R.; Green, S. *Curr. Top. Med. Chem.* **2005**, *5*, 199.
8. Heron, N. M.; Anderson, M.; Blowers, D. P.; Breed, J.; Eden, J. M.; Green, S.; Hill, G. B.; Johnson, T.; Jung, F. H.; McMiken, H. H. J.; Mortlock, A. A.; Pannifer, A. D.; Pauptit, R. A.; Pink, J.; Roberts, N. J.; Rowsell, S. *Bioorg. Med. Chem. Lett.* **2006**, *16*, 1320.
9. Jung, F. H.; Pasquet, G.; Lambert-van der Brempt, C.; Lohmann, J.-J. M., et al. *J. Med. Chem.* **2006**, *49*, 955.
10. Zhang, Q.; Liu, Y.; Gao, F.; Ding, Q.; Cho, C.; Hur, W.; Jin, Y.; Uno, T.; Joazeiro, C. A. P.; Gray, N. *J. Am. Chem. Soc.* **2006**, *128*, 2182.
11. Noble, M. E. M.; Endicott, J. A.; Johnson, L. N. *Science* **2004**, *303*, 1800.
12. Anderson, M.; Beattie, J. F.; Breault, G. A.; Breed, J.; Byth, K. F.; Culshaw, J. D.; Ellston, R. P.; Green, S.; Minshull, C. A.; Norman, R. A.; Pauptit, R. A.; Stanway, J.; Thomas, A. P.; Jewsbury, P. J. *Bioorg. Med. Chem. Lett.* **2003**, *13*, 3021.
13. Tavares, F. X.; Boucheron, J. A.; Dickerson, S. H.; Griffin, R. J.; Preugschat, F.; Thomson, S. A.; Wang, T. Y.; Zhou, H.-Q. *J. Med. Chem.* **2004**, *47*, 4716.
14. Wang, S.; Meades, C.; Wood, G.; Osnowski, A.; Anderson, A.; Yuill, R.; Thomas, M.; Mezna, M.; Jackson, W.; Midgley, C.; Griffiths, G.; Fleming, I.; Green, S.; McNae, I.; Wu, S.-Y.; McInnes, C.; Zheleva, D.; Walkinshaw, M. D.; Fischer, P. M. *J. Med. Chem.* **2004**, *47*, 1662.
15. The Aurora A kinase domain was expressed in BL21(DE3) cells using a modified pET28 expression vector. The sequence of the final purified protein was identical to the protein described in reference 16. The final protein buffer contained 50 mM Tris, pH 8.0, 0.5 mM EDTA, 1 mM DTT, and 200 mM NaCl. For crystallization, 0.5 mM compound **1** (purchased from Calbiochem) was added AIK concentrated to 5 mg/ml. For crystallization, hanging drop vapor diffusion was employed (20 °C), using drops containing a 1:1 ratio of the concentrated protein solution and a reservoir comprising 7% (w/v) PEG 400, 2.2 M ammonium sulfate and 100 mM Hepes, pH 7.5. Crystals were cryoprotected by brief immersion in the reservoir solution supplemented with 20% (v/v) ethylene glycol, harvested in nylon loops and frozen in liquid nitrogen for data collection. X-ray data were collected at beamline 4.2.2 at the ALS, Berkeley, at 10000 eV on a Noirl CCD detector. Data were analysed and reduced using d\*TREK<sup>23</sup> and CCP4.<sup>24</sup>
16. Nowakowski, J.; Cronin, C. N.; McRee, D. E.; Knuth, M. W.; Nelson, C. G.; Pavletich, N. P.; Rogers, J.; Sang, B.-C.; Scheibe, D. N.; Swanson, R. V.; Thompson, D. A. *Structure* **2002**, *10*, 1659.
17. The molecular replacement calculations were carried using PHASER in the CCP4 suite.<sup>24</sup>
18. The structure was refined using REFMAC in the CCP4 suite.<sup>24</sup> All electron density map visualization and manual model rebuilding were carried out using the XtalView/Xfit package.<sup>25</sup> The PDB accession code is 2NP8.
19. Bayliss, R.; Sardon, T.; Vernos, I.; Conti, E. *Mol. Cell* **2003**, *12*, 851.
20. Cheetham, G. M. T.; Knechtal, R. M. A.; Coll, J. T.; Renwick, S. B.; Swenson, L.; Weber, P.; Lippke, J. A.; Austen, D. A. *J. Biol. Chem.* **2002**, *277*, 42419.
21. Young, M. A.; Shah, N. P.; Chao, L. H.; Seeliger, M.; Milanov, Z. V.; Biggs, W. H.; Treiber, D. K.; Patel, H. K.; Zarrinkar, P. P.; Lockhart, D. J.; Sawyers, C. L.; Kuriyan, J. *Cancer Res.* **2006**, *66*, 1007.
22. Harrington, E. A.; Bebbington, D.; Moore, J.; Rasmussen, R. K.; Ajose-Adeogun, A. O.; Nakayama, T.; Graham, J. A.; Demur, C.; Hercend, T.; Diu-Hercend, A.; Su, M.; Golec, J. M. C.; Miller, K. M. *Nat. Med.* **2004**, *10*, 262.
23. Pflugrath, J. W. *Acta Crystallogr.* **1999**, *D55*, 1718.
24. CCP4 (Collaborative Computational Project, No. 4), *Acta Crystallogr.* **1994**, *D50*, 760.
25. McRee, D. E. *J. Struct. Biol.* **1999**, *125*, 156.